Optimal control of a turbulent fibre suspension flowing in a planar contraction

Raino A. E. Mäkinen*and Jari Hämäläinen†

2006

Abstract

Fibre orientation distribution of a turbulent fibre suspension flowing in a planar contraction is considered. The fibre orientation is modeled using a diffusion–convection type equation while the average flow velocity of the suspension is modeled using a simple one-dimensional model. Our aim is to control the fibre orientation distribution at the end of the contraction by changing its shape. The shape is discretized with Bezier function and the diffusion–convection equation with SUPG finite element method. Algebraic sensitivity analysis for the discretized optimization problem is done with the aid of automatic differentiation techniques. Numerical examples are given.

KEY WORDS: *fibre suspension flow, fibre orientation, finite element method, design optimization, sensitivity analysis*

This is the final draft for paper that appeared in: Commun. Numer. Meth. Engng. (22) 567-–575, 2006. DOI: 10.1002/cnm.833

1 Introduction

Paper is an anisotrophy material produced from a fiber suspension by a papermaking machine. The basic structure of a paper is formed at the wet-end of the paper machine. A mixture of water, wood fibers and some other papermaking substances flows through a headbox slice channel and continues to a forming section. The headbox slice channel is a contracting nozzle and thus, it accelerates the fluid velocity to a machine speed. After a free jet from the headbox to the forming section, most of the water is removed and basic solid structure of the paper is formed.

A fiber orientation distribution determines strength properties of the paper. A random fiber orientation distribution would result in an equal tensile strength both in a machine direction (MD) and in a cross-machine direction (CD). The equal tensile strengths are important for some paper grades, but in practice, the paper is allowed to be stronger in MD than in CD in order to have good runnability of a paper machine (a strong paper in MD helps in running the machine faster resulting in more production). But, the tensile strength ratio cannot be too high. Otherwise end-use properties of the paper during printing processes or in copying machines would be too much deteriorated.

A speed difference between the headbox jet and moving wires of the forming section affect on the fiber orientation of the produced paper, but the initial fiber orientation distribution is essential for practical papermaking. In fact, the jet-to-wire ratio can easily be controlled in a paper machine, but the initial fiber orientation distribution is determined by the design of the headbox slice channel fluid dynamics in the nozzle.

A mathematical model for the fibre orientation distribution is based on a work done by Jeffery in early 1920's [8]. He studied an ellipsoidal particle moving in a Stokes flow, assuming an inertialess

*Dept. of Math. Information Technology, P.O. Box 35 (Agora), FI-40014 University of Jyväskylä, Finland
†Department of Applied Physics, University of Kuopio, P.O. Box 1627, FI-70211 Kuopio, Finland

particle and constant fluid velocity gradient. The theory is later extended to more complex shear flows, see for example [15] and [9]. An extended review on the fibre orientation modeling can be found in [14].

The fibre orientation distribution model has been numerically solved and experimentally validated in [7] and [13]. It was shown that the contracting nozzle and accelerated flow directs the fibers into the main flow direction resulting in non-uniformly distributed fibers. An effect of so-called turbulence vanes (located inside the nozzle) on fiber orientation distribution was also shown in [7]. Thus, it is obvious that the design and resulting fluid dynamics controls the fiber orientation distribution.

In this paper our goal is to formulate and solve an optimal control problem such that the fiber orientation distribution will be as random as possible at the end of the nozzle. The distribution is controlled by an optimal shape design of the contraction. In this paper we do not consider practical machine construction problems, but we show that the fiber orientation distribution can be controlled optimally by the design. The optimized design is not necessarily directly applicable in practice, but it gives fresh ideas to engineers how to develop the design.

2 Fibre orientation model for a one-dimensional headbox

A simplified model of the orientation distribution of fibres moving through the headbox was derived in [13]. The geometry of the planar contraction (one-dimensional headbox) of varying height 2α is shown in Figure 1. The one-dimensional headbox problem considers only the mean translation of the fibres along the central streamline. The model only considers the distribution of the projected angle ϕ of the fibre. The problem is further simplified by assuming one-dimensional steady flow $\vec{u} = (u_1(x_1), 0)$. The problem is made dimensionless by scaling variables by the headbox length L and inlet velocity $u_1(0)$.

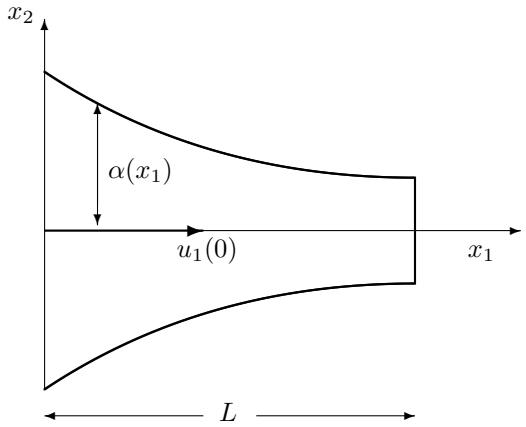

Figure 1: Geometry of the one-dimensional headbox

The probability distribution of projected angle ϕ at point x_1 is denoted by $\Psi(x_1, \phi)$ and is given as the solution of the linear diffusion–convection type problem in domain $\Omega =]0, 1[\times] - \frac{\pi}{2}, \frac{\pi}{2}[$:

$$-\nabla \cdot \mathcal{A}\nabla\Psi + \boldsymbol{b} \cdot \nabla\Psi + c\Psi = 0 \qquad \text{in } \Omega. \tag{1}$$

The coefficients of the problem are given by

$$\mathcal{A} = \begin{bmatrix} D_T & 0 \\ 0 & D_R \end{bmatrix}, \quad \boldsymbol{b} = \left(u_1, -\sin(2\phi)\frac{\partial u_1}{\partial x_1} \right)^{\mathrm{T}}, \quad c = -2\cos(2\phi)\frac{\partial u_1}{\partial x_1},$$

where D_T, D_R are given positive constants: the translational dispersion coefficient and rotational dispersion coefficient, respectively.

At the headbox inlet to the contraction, we assume that fibres are randomly oriented, i.e. we have the Dirichlet boundary condition

$$\Psi = \pi^{-1} \quad \text{on } \Gamma_1 := \{0\}\times]-\frac{\pi}{2},\frac{\pi}{2}[. \tag{2}$$

At the outlet and for the angles $\phi = \pm\frac{\pi}{2}$ we impose homogeneous Neumann boundary condition

$$\frac{\partial \Psi}{\partial n} = 0 \quad \text{on } \Gamma_2 \cup \Gamma_3, \tag{3}$$

where $\Gamma_2 = \{1\}\times]-\frac{\pi}{2},\frac{\pi}{2}[$, $\Gamma_3 = \partial\Omega \setminus \overline{(\Gamma_1 \cup \Gamma_2)}$.

For more fluid dynamical aspects of the fibre orientation distribution model and numerical simulation results we refer to [7] and [13]. Especially, the model is solved together with a realistic fluid dynamical model, that is, the full two-dimensional Navier-Stokes equations and a turbulence model, in [7] for different headbox constructions by varying turbulence vanes inside the nozzle.

3 The shape optimization problem

Our aim is to find a shape of the contraction such that the orientations of fibres at the outlet would be evenly distributed. Therefore the variable height of the contraction becomes the control variable. We define the following set of admissible controls:

$$U^{ad} = \left\{ \alpha \in C^{1,1}([0,1]) \mid \hat{\alpha} \le \alpha \le \hat{\hat{\alpha}} \text{ in } [0,1],\ \left|\frac{d\alpha}{dx_1}\right| \le c \text{ in }]0,1[\right\},$$

where $\hat{\alpha}, \hat{\hat{\alpha}}$ are positive C^1-functions and c is a given positive constant.

To calculate the mean translational and rotational velocity of the fibre, the mean flow field in the planar contraction along the central streamline $x_2 = 0$ needs to be defined. For an incompressible, one-dimensional flow $\vec{u} = (u_1(x_1), 0)$ continuity implies

$$u_1(x_1)2\alpha(x_1) = \text{constant}.$$

Thus the velocity in x_1 direction is given by

$$u_1(x_1) = \frac{u_1(0)\alpha(0)}{\alpha(x_1)} =: \beta\frac{1}{\alpha(x_1)},$$

implying that the flow field is eliminated from the fibre orientation model.

To give the weak formulation of (1)–(3) we introduce the following sets of functions

$$V = \{v \in H^1(\Omega) \mid v = 0 \text{ on } \Gamma_1\},$$
$$V_g = \{v \in H^1(\Omega) \mid v = \pi^{-1} \text{ on } \Gamma_1\}.$$

The weak formulation of (1)–(3) then reads as follows

$$\begin{cases} \text{Find } \Psi := \Psi(\alpha) \in V_g \text{ such that} \\ \displaystyle\int_\Omega (\mathcal{A}\nabla\Psi \cdot \nabla v + (\boldsymbol{b}(\alpha)\cdot\nabla\Psi)v + c(\alpha)\Psi v)\, dx = 0 \quad \forall v \in V, \end{cases} \tag{$\mathcal{P}(\alpha)$}$$

where $\boldsymbol{b}(\alpha) = (\beta\alpha^{-1},\ \beta\sin(2\phi)\alpha^{-2}\frac{d\alpha}{dx_1})$ and $c(\alpha) = 2\beta\cos(2\phi)\alpha^{-2}\frac{d\alpha}{dx_1}$.

Our aim is to find a function α such that the fibre orientation distribution at the outlet is close to a given target distribution $\Psi_0 \in L^2(\Gamma_2)$. Therefore we formulate the following PDE constrained optimization problem:

$$\begin{cases} \text{Find } \alpha^\star \in U^{ad} \quad \text{such that} \\ J(\Psi(\alpha^\star)) \le J(\Psi(\alpha)) \quad \forall \alpha \in U^{ad}, \end{cases} \tag{$\mathbb{P}$}$$

where

$$J(\Psi(\alpha)) = \int_{\Gamma_2} (\Psi(\alpha) - \Psi_0)^2 \, ds$$

with $\Psi(\alpha)$ being the solution to $(\mathcal{P}(\alpha))$.

We note that problem $(\mathbb{P})$ is an optimal control problem with control in coefficients. No variable domains are involved in the problem.

4 Numerical realization

Instead of the original infinite dimensional optimal control problem $(\mathbb{P})$ we shall solve numerically an approximate mathematical programming problem. Therefore we shall discretize both the admissible set of controls and the state problem.

Let U_n^{ad} be a discretization of U^{ad} by Bezier functions

$$\alpha_n(x_1) = \sum_{i=0}^{n-1} a_{i+1} \binom{n}{i} (1 - x_1)^{n-i} x_1^i, \tag{4}$$

where $\boldsymbol{a} = (a_1, ..., a_n)^{\mathrm{T}} \in \mathcal{U}$. Here $\mathcal{U} \subset \mathbb{R}^n$ is chosen in such a way that $\boldsymbol{a} \in \mathcal{U} \iff \alpha_n \in U_n^{ad}$. Thus, the parameter vector to be optimized is $\boldsymbol{a}$.

Let $\Omega = \cup_e \Omega_e$ be a partition of the rectangular domain Ω into rectangular elements. We define the following finite element spaces

$$V_h = \{v_h \in V \mid v_h|_{\Omega_e} \in Q_1 \ \forall \Omega_e \in \mathcal{T}_h, \ v_h|_{\Gamma_1} = 0\},$$
$$V_{gh} = \{v_h \in V \mid v_h|_{\Omega_e} \in Q_1 \ \forall \Omega_e \in \mathcal{T}_h, \ v_h|_{\Gamma_1} = \pi^{-1}\}.$$

The state problem $(\mathcal{P}(\alpha))$ is approximated using streamline upwind Petrov–Galerkin (SUPG) method [1]

$$\begin{cases} \text{Find } \Psi_h := \Psi_h(\boldsymbol{a}) \in V_{gh} \text{ such that} \\ \displaystyle\int_\Omega (\mathcal{A}\nabla\Psi_h \cdot \nabla v_h + (\boldsymbol{b} \cdot \nabla\Psi_h) v_h + c\Psi_h v_h) \, dx + \sum_e \int_{\Omega_e} \tau_h^{(e)} (\boldsymbol{b} \cdot \nabla\Psi_h + c\Psi_h) \boldsymbol{b} \cdot \nabla v_h \, dx = 0 \quad \forall v_h \in V_h. \end{cases} \tag{5}$$

Above $\tau_h^{(e)} > 0$ is an upwinding parameter depending on the local Peclet number.

Let h be fixed and let $\{\varphi_i\}$ be the set of Lagrangian basis functions of V_h. Then $\Psi_h = \sum_{i=1}^N q_i \varphi_i$, where $\boldsymbol{q} = (q_1, \ldots, q_N)^{\mathrm{T}}$ contain the nodal values of Ψ_h. The matrix formulation of (5) leads to a system of linear algebraic equations

$$\boldsymbol{R}(\boldsymbol{a}, \boldsymbol{q}(\boldsymbol{a})) = \boldsymbol{0}. \tag{6}$$

The residual vector $\boldsymbol{R}(\boldsymbol{a}, \boldsymbol{q})$ is assembled element-by-element in the usual way:

$$\begin{aligned} &\boldsymbol{R}(\boldsymbol{a}, \boldsymbol{q}) = \sum_{ass.} \boldsymbol{R}^e(\boldsymbol{a}, \boldsymbol{q}(\boldsymbol{a})) \\ &\boldsymbol{R}_i^e(\boldsymbol{a}, \boldsymbol{q}) := \int_{\Omega_e} (\mathcal{A}\nabla\Psi_h \cdot \nabla\varphi_i + (\boldsymbol{b}(\boldsymbol{a}) \cdot \nabla\Psi_h)\tilde{\varphi}_i + c(\boldsymbol{a})\Psi_h\tilde{\varphi}_i) \, dx, \quad \tilde{\varphi}_i := \varphi_i + \tau_h^{(e)} \boldsymbol{b}(\boldsymbol{a}) \cdot \nabla\varphi_i \end{aligned} \tag{7}$$

The matrix form of the cost function reads as

$$\mathcal{J}(\boldsymbol{q}(\boldsymbol{a})) = \sum_e \int_{\partial\Omega_e \cap \Gamma_2} \big(\sum_i q_i \varphi_i - \Psi_0\big)^2 \, ds. \tag{8}$$

Finally, we have the following mathematical programming problem:

$$\begin{cases} \text{Find } \boldsymbol{a}^\star \in \mathcal{U} \text{ such that} \\ \mathcal{J}(\boldsymbol{q}(\boldsymbol{a}^\star)) \le \mathcal{J}(\boldsymbol{q}(\boldsymbol{a})) \quad \forall \boldsymbol{a} \in \mathcal{U}, \end{cases} \tag{9}$$

where $\boldsymbol{q}(\boldsymbol{a})$ is the solution of (6).

The set $\mathcal{U}$ is compact and the mapping $\boldsymbol{a} \mapsto \mathcal{J}(\boldsymbol{q}(\boldsymbol{a}))$ is clearly continuous, therefore there exist a minimizer $\boldsymbol{a}^\star$. If the chosen upwing parameter depends smoothly on the coefficients of the problem, then by the Implicit Function Theorem the mapping $\boldsymbol{a} \mapsto \mathcal{J}(\boldsymbol{a})$ is smooth. Therefore one may utilize standard descent methods to approximate a local minimizer.

To be able to use descent methods requiring exact gradient information for the numerical solution of (9) we need to perform the algebraic sensitivity analysis on it. The partial derivative of $\mathcal{J}$ at $\boldsymbol{a}$ with respect to a_k is given by

$$\frac{\partial \mathcal{J}(\boldsymbol{q}(\boldsymbol{a}))}{\partial a_k} = -\boldsymbol{p}^{\mathrm{T}} \left(\frac{\partial \boldsymbol{R}(\boldsymbol{a}, \boldsymbol{q})}{\partial a_k} \right), \quad k = 1, ..., n, \tag{10}$$

where $\boldsymbol{p} := \boldsymbol{p}(\boldsymbol{a})$ solves the adjoint equation

$$\left(\frac{\partial \boldsymbol{R}(\boldsymbol{a}, \boldsymbol{q})}{\partial \boldsymbol{q}} \right)^{\mathrm{T}} \boldsymbol{p} = \nabla_{\boldsymbol{q}} \mathcal{J}(\boldsymbol{q}) \tag{11}$$

and $\frac{\partial \boldsymbol{R}}{\partial \boldsymbol{q}}$ denotes the partial Jacobian of $\boldsymbol{R}(\boldsymbol{a}, \boldsymbol{y})$ with respeact to $\boldsymbol{y}$ at $(\boldsymbol{a}, \boldsymbol{q}(\boldsymbol{a}))$.

5 Numerical examples

Next we present two numerical examples related to two different values of the rotational dispersion coefficient D_R. Due to symmetry, the actual computational domain consist of only half of the domain Ω corresponding to angles $0 < \phi < \frac{\pi}{2}$. The finite element mesh contains 4800 rectangular bilinear elements. The mesh is refined near $\phi = 0$ in order to capture high gradients of fibre orientation angle. The function characterizing the height of the contraction is discretized by a Bezier function with 40 control points. The parameters defining the set U^{ad} are

$$\hat{\alpha}(x_1) = 0.1 - 0.33x_1 + 0.345x_1^2 - 0.105x_1^3, \quad \hat{\hat{\alpha}}(x_1) = 0.1(1 - x_1) + 0.01x_1, \quad c = 10.$$

The target distribution is $\Psi_0(\phi) \equiv \pi^{-1}$. Other geometrical and physical parameters have (dimensionless) values $u(x_1) = 0.1/\alpha(x_1)$, $D_T = 0.00001$,

The numerical results were computed using a finite element analysis (and optimization) package "Numerrin 2.0" [5]. In this software package, the partial derivatives in (11) and the right-hand side of (10) are obtained using automatic differentation technique ([4]) applied on the local (element) contributions in (7), (8). In this way, the natural sparsity of the problem will be taken into account and rather simple implementation of the automatic differentiation technique is adequate. For further details, see [6], [11]. The optimization module of Numerrin 2.0 uses an implementation of the sequential quadratic programming (SQP) method (see e.g. [2]) to find a local minimum for problem (9). In the implementation, the QP subproblem is solved using the method due to Goldfarb and Idnani [3].

We first solved the optimization problem for $D_R = 5$. The initial guess was equal to the traditional linearly tapered design $\hat{\hat{\alpha}}$. After 25 iterations, the value of the cost function was reduced from 0.552×10^0 to 0.827×10^{-3}. The final geometry of the contraction is shown in Figure 2 together with the initial and final orientation distributions at the outlet. Also, the constraint functions $\hat{\alpha}$, $\hat{\hat{\alpha}}$ and the target distribution Ψ_0 are shown in Figure 2.

Contour plots of the initial and final orientation distributions in the whole computational domain are shown in Figure 3. The horizontal direction is the machine direction (flow direction), and the vertical one is the propability axis.

The same problem was then solved for $D_R = 0.5$. The initial guess was again equal to the linearly tapered design. After 21 iterations, the value of the cost function was reduced from 0.268×10^1 to 0.888×10^{-1}. The final geometry of the contraction is shown in Figure 4 together with the initial and final orientation distributions at the outlet. Contour plots of the initial and final orientation distributions in the whole computational domain are shown in Figure 5.

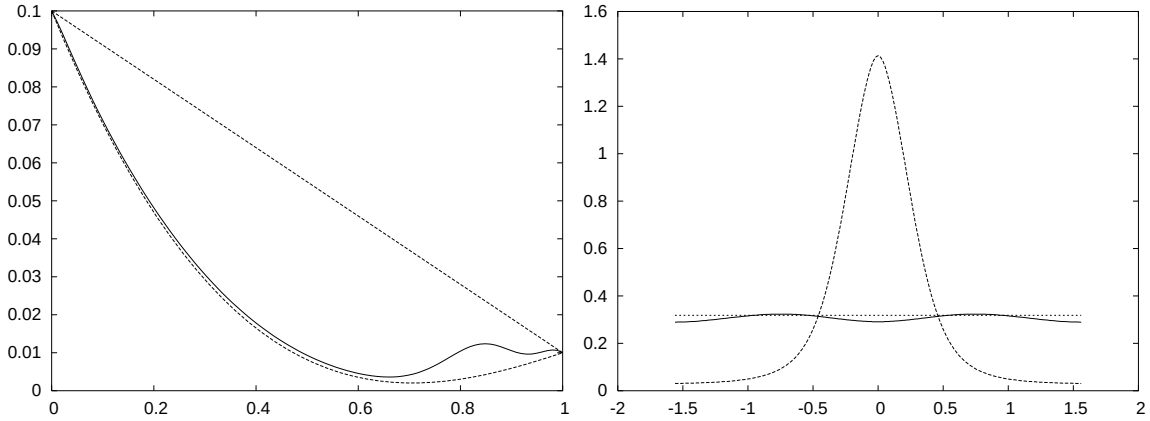

Figure 2: Initial/final heights (left) and propablity distributions (right) at the end of the contraction

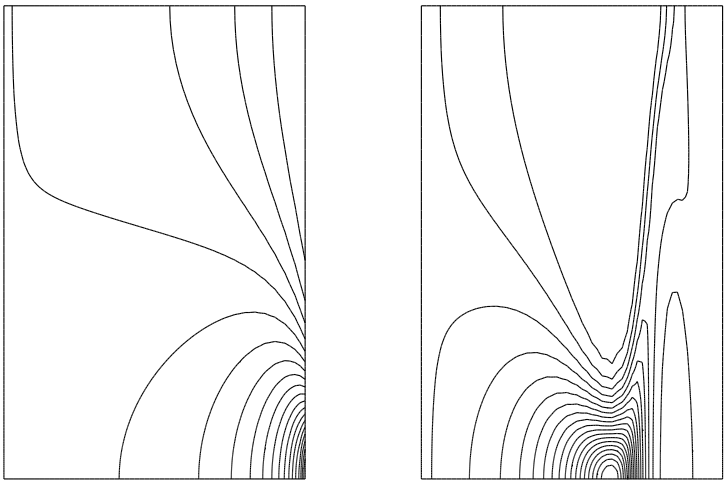

Figure 3: Contour plot of Ψ_h corresponding to the initial and the final contraction shape

There is no guarrantee that the cost function is unimodal, so the computed optimums are possibly only local ones. However, we took several random initial guesses and ended up to same results. Thus, there are good chances that the final designs really represent global optima.

One can see that the optimum design is quite far from the traditional linearly tapered design. Two questions immediately rises: Does the computed optimum design correspond practically realizable design? Can we alternatively interpret the variations of height of the contraction as the insertion of effectively similar vanes in the traditional design? These questions will be studied in future research projects.

6 Conclusions

In this study, the orientation distribution of fibres in a turbulent suspension passing through a planar contraction was optimized by controlling the shape of the contraction. The fibre orientation distribution was modeled using diffusion–convection type partial differential equation. For fluid flow a very simple model was used that allowed us to eliminate flow field from the optimization problem.

The rigorous mathematical analysis of the existence of solution to ($\mathbb{P}$) and the convergence of approximate solutions will be done in a forthcoming paper. In the near future, our aim is to replace

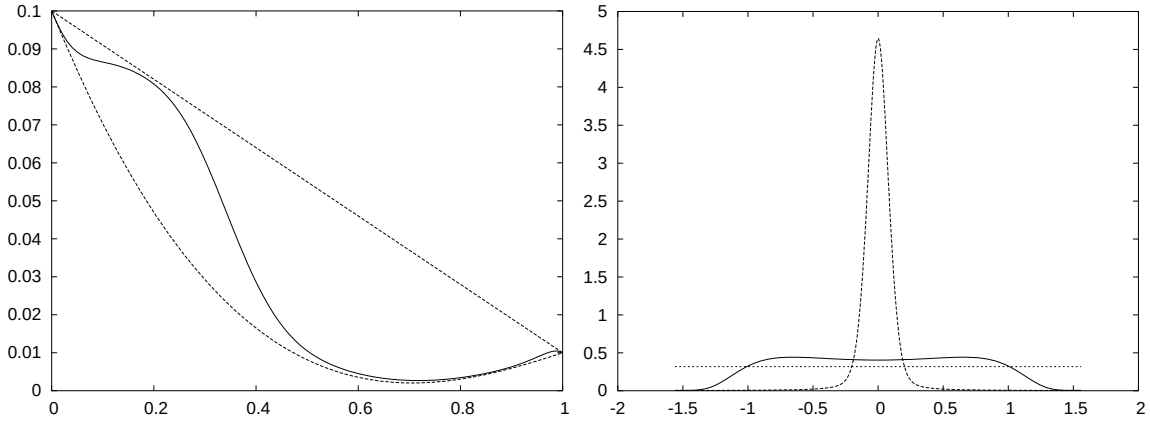

Figure 4: Initial/final heights (left) and propablity distributions (right) at the end of the contraction

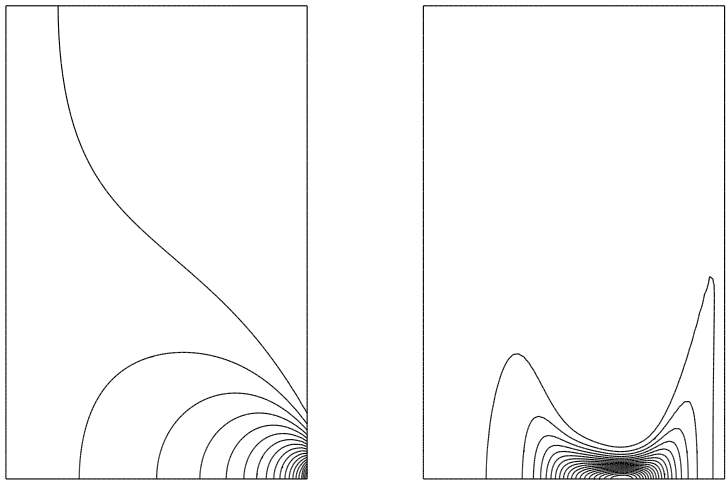

Figure 5: Contour plot of Ψ_h corresponding to the initial and the final contraction shape

the simple one-dimensional ideal flow model with more realistic Navier–Stokes model.

Numerical examples given in this paper show that it is possible to control the fibre orientation distribution by the contraction shape. In fact, almost random distribution was obtained. The optimized design is not necessary desired in real industrial applications, but surely this paper shows that it is possible to control the fibre orientation distribution. By developing more realistic Navier–Stokes model and formulating more practical target functions and constraits, it is possible to search also industrially relevant new design.

References

[1] Brooks AN, Hughes TRJ. Streamline upwind/Petrov–Galerkin formulations for convection dominated flows with particular emphasis on the incompressible Navier-Stokes equations, *Comput. Meth. Appl. Mech. Eng.* 1982; **32**: 199–259.

[2] Gill PE, Murray W, Wright MH. *Practical Optimization*, Academic Press: New York, 1981.

[3] Goldfarb D, Idnani A. A numerically stable dual method for solving strictly convex quadratic programs, *Mathematical Programming* 1983; **27**: 1–33.

[4] Griewank A. *Evaluating Derivatives, Principles and Techniques of Algorithmic Differentiation*, SIAM: Philadelphia, 2000.

[5] Hiltunen K, Laitinen M, Niemistö A, Tarvainen P, Using mathematical concepts in software design of computational mechanics, In *Proceedings of VIII Finnish Mechanics Days*, 2003.

[6] Haslinger J, Mäkinen RAE. *Introduction to Shape Optimization: Theory, Approximation, and Computation*, SIAM: Philadelphia, 2003.

[7] Hyensjö M, Krochak P, Olson J, Hämäläinen J, Dahlkild A. Modelling a turbulent dilute fibre suspension in a planar contraction: Effect of vane types, vane position and wall boundary layer on fibre orientation distribution, In *5th International Conference on Multiphase Flow, ICMF'04*, Paper No.436, Yokohama, Japan, 2004.

[8] Jeffery G. The motion of ellipsoidal particles immersed in a visous fluid, *Proc. R. Soc. Lond.* 1922; A102: 161.

[9] Kagermann H, Köhler W. On the motion of nonspherical particles in a turbulent flow, *Physica* 1984; 116A: 178–198.

[10] Hämäläinen J, Mäkinen RAE, Tarvainen P. Optimal design of paper machine headboxes, *Int. J. Numer. Meth. Fluids* 2000; **34**: 685–700.

[11] Mäkinen RAE. Simple automatic derivatives in shape optimization, In *Proceedings of 4th European Congress on Computational Methods in Applied Sciences and Engineering*, CD-ROM, vol. II, P. Neittaanmäki, T. Rossi, S. Korotov, E. Onate, J. Periaux, and D. Knörzer (eds.), 2004.

[12] Mohammadi B, Pironneau O. *Applied Shape Optimization for Fluids*, Oxford University Press: Oxford, 2001.

[13] Olson JA, Frigaard I, Chan C, Hämäläinen JP. Modeling a turbulent fibre suspension flowing in a planar contraction: The one-dimensional headbox, *Int. J. Multiphase Flow* 2004; **30**: 51–66.

[14] Olson J, Kerekes RJ. The motion of fibres in turbulent flow, *J. Fluid Mech*, 1988; **377**, 47–64.

[15] Shanker R, Gillespie Jr. JW, Guceri SI. On the effect of nonhomogeneous flow fields on the orientation distribution and rheology of fibre suspensions, *Polym. Eng. Sci.* 1991; **31**: 161–171.